## Improved Lanczos Algorithm using Matrix Product States

Yu Wang  $0^{\S}, 1, *$  Zhangyu Yang  $0^{\S}, 2, \dagger$  and Christian B. Mendl  $0^{1,3, \ddagger}$ 

<sup>1</sup> Technical University of Munich, CIT, Department of Computer Science, Boltzmannstraße 3, 85748 Garching, Germany
 <sup>2</sup> Technical University of Munich, Department of Physics, 85748 Garching, Germany
 <sup>3</sup> Technical University of Munich, Institute for Advanced Study, Lichtenbergstraße 2a, 85748 Garching, Germany
 (Dated: May 1, 2025)

We improve the Lanczos algorithm using the matrix product state representation proposed in Phys. Rev. B 85, 205119 (2012). As an alternative to the density matrix renormalization group (DMRG), the Lanczos algorithm avoids local minima and can directly find multiple low-lying eigenstates. However, its performance and accuracy are affected by the truncation required to maintain the efficiency of the tensor network representation. In this work, we enhance its convergence by restarting with multiple states. We benchmark our method on one-dimensional instances of the Fermi–Hubbard model with 8 sites and the Heisenberg model with 16 sites in an external field, using numerical experiments targeting the first five lowest eigenstates. Across these tests, our approach obtains accuracy improvements of three to seven orders of magnitude. Finally, we extend the Heisenberg model simulation to a lattice with 30 sites to highlight its scalability.

## I. INTRODUCTION

Eigenvalue problems lie at the heart of quantum many-body physics, materials science, and quantum chemistry. By finding a few low-lying eigenstates of the Hamiltonian, one can access ground-state properties [1–5], low-temperature thermodynamics [6–9], and dynamical correlation functions [10–12]. The Lanczos algorithm [1, 13–19] is widely used to find the low-lying eigenstates of large linear systems, and is implemented in popular packages like ARPACK [20]. Nevertheless, its capability is limited by the curse of dimensionality for many-body quantum systems, as the Hilbert space dimension grows exponentially with the system size.

Tensor network methods [21–27] representing quantum states and operators by matrix product states (MPS) and matrix product operators (MPO) significantly alleviate this issue. As a key insight, the low-lying states only stay in a small corner of the whole Hilbert space due to the area law of the entanglement entropy, allowing them to be efficiently approximated by low-rank decompositions like MPS. The density-matrix renormalizationgroup (DMRG) algorithm exploits these properties and optimizes an MPS ansatz variationally. However, DMRG is essentially a local energy minimizer: it may become trapped in local minima [28, 29]; also, it does not have direct access to the excited states. The Lanczos algorithm, by contrast, naturally produces a spectrum of Ritz pairs and inherently avoids local minima when initialized with the proper initial state. The combination of the Lanczos algorithm and tensor network offers a promising complementary approach for exploring the low-lying eigenstates of large-scale quantum many-body systems [30].

Unfortunately, using tensor network representations for the Lanczos algorithm introduces a new bottleneck: generating new Krylov vectors enlarges the bond dimensions, so MPS compression is required to keep the calculation feasible and efficient. The MPS truncation introduces non-negligible errors, which result in two significant issues. First, this error causes a loss of orthogonality among the Krylov vectors. A post-reorthogonalization technique [30] has been developed to address this issue. Second, because each Krylov vector depends on its predecessors, the truncation error accumulates as the subspace is generated. This accumulation causes the Krylov subspace to diverge from the ideal one and prevents it from introducing new independent information. As discussed later in Sec. IIC, the resulting convergence stalls at a much higher error level than expected.

In this work, we focus on the second issue and improve the convergence of the tensor network-based Lanczos algorithm. Restarting the Lanczos process with a Ritz vector can perpetuate its convergence. Nevertheless, targeting multiple eigenstates remains challenging and expensive. To address this issue, we further refine the algorithm by introducing a multi-state restart Lanczos (MRL) scheme in which multiple Ritz vectors are utilized to accelerate the convergence. Compared with a single-state restart, MRL recycles spectral information that would otherwise be discarded, dramatically reducing the total number of Krylov vectors required to converge the target states, while achieving higher accuracy beyond the simple single-state restart.

We benchmark our algorithm on the half-filled Fermi–Hubbard chain and the spin-1/2 Heisenberg XXZ model in a longitudinal magnetic field in Sec. IV. For both cases, MRL significantly improves the accuracy by three to seven orders of magnitude while staying economical. To examine its scalability, we also apply our approach to a larger Heisenberg XXZ chain of size L=30.

While preparing this manuscript, we became aware of a recent work by Dektor et al. [31] that exploits a similar intuition, namely, that incorporating Ritz vectors into

<sup>\* 18</sup>yu.wang@tum.de

<sup>†</sup> zhangyu.yang@tum.de

<sup>‡</sup> christian.mendl@tum.de

<sup>§</sup> These authors contributed equally to this work.

the iteration can significantly reduce truncation error. Dektor et al. employ a different routine, the subspace iteration, to make this intuition practical.

#### II. THEORETICAL BACKGROUND

### A. The Lanczos algorithm

The Lanczos algorithm is a widely used iterative method for computing the extremal eigenpairs of Hermitian matrices [1, 13, 14, 32], and has been widely used in diagonalizing large Hamiltonians within quantum many-body physics [33, 34]. Starting with a proper initial normalized state  $|v_0\rangle$ , the Lanczos algorithm confines the evolving space to the Krylov subspace spanned by  $\{|v_0\rangle, H|v_0\rangle, H^2|v_0\rangle, \dots, H^{k-1}|v_0\rangle\}$ . The Lanczos procedure recursively constructs the Krylov vectors via a three-term recurrence relation:

$$|w_i\rangle = H|v_{i-1}\rangle,\tag{1a}$$

$$|w_{j}'\rangle = |w_{j}\rangle - |v_{j-1}\rangle \langle v_{j-1}|w_{j}\rangle - |v_{j-2}\rangle \langle v_{v-2}|w_{j}\rangle,$$
 (1b)

$$|v_j\rangle = |w_j'\rangle/\||w_j'\rangle\|,\tag{1c}$$

for j > 1. The new Krylov vector  $|v_j\rangle$  is formed by applying H to  $|v_{j-1}\rangle$ , orthogonalizing it against the two previous Krylov vectors with the Gram-Schmidt process [35] in Eq. (1b), and finally normalizing the result by Eq. (1c). One only needs to orthogonalize the vector against  $v_0$  for j = 1.

This iteration builds an orthonormal basis of the Krylov subspace  $V = \text{span}\{|v_0\rangle, |v_1\rangle, \cdots, |v_{k-1}\rangle\}$ . Projecting the original Hamiltonian H onto the subspace V yields a reduced (effective) Hamiltonian, whose elements are given by:

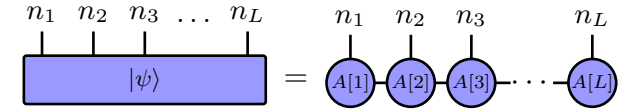
$$\tilde{H}_{ij} = \langle v_i | H | v_j \rangle. \tag{2}$$

Diagonalizing this  $k \times k$  matrix  $\tilde{H}$  yields the approximated eigenvalues  $(\theta_i)_{i=1,\dots,k}$  together with the coefficient vectors  $(\mathbf{y}_i)_{i=1,\dots,k}$ . The approximation to the exact eigenvectors of the original Hamiltonian H is reconstructed by back-transformation:

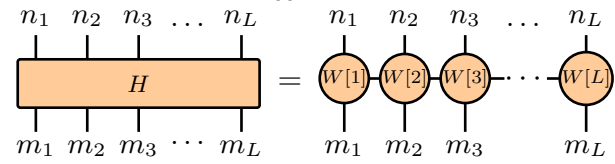
$$|R_i\rangle = \sum_{j=0}^{k-1} (\mathbf{y}_i)_j |v_j\rangle.$$
 (3)

The quantities  $\theta_i$  and  $|R_i\rangle$  are called the Ritz value and Ritz vector, respectively. After the set of Ritz pairs  $\{\theta_i, |R_i\rangle\}$  is obtained, each pair is tested for convergence; those that meet a desired tolerance of convergence are accepted as the numerical eigenpairs of H [15, 36].

For many physically or chemically relevant Hamiltonians, only a few dozen or hundred basis vectors  $(k \ll \dim(\mathcal{H}))$  already yield accurate low-lying eigenstates [30, 32, 37], and only these k Krylov vectors need to be stored. The Lanczos algorithm turns a huge eigenvalue problem into a much smaller one inside the Krylov subspace, making it attractive for computational physics.



(a) The wavefunction is obtained by contracting the "tensor train" made of matrices  $A[i]^{n_i}$ .



(b) MPO ansatz for an L-site chain, the operator can be reconstructed by contracting all the local matrices  $W[i]^{m_i n_i}$ .

Figure 1: Diagrammatic representation of matrix product states and operators.

### B. Matrix product states and operators

Even though the Lanczos algorithm significantly reduces the complexity of the eigenvalue problem, it still runs into the curse of dimensionality issue since the memory needed to store the vectors (wavefunctions) explicitly scales exponentially with the system size.

Therefore, it is beneficial to employ the tensor network representation [21, 22, 38, 39], especially the matrix product state (MPS) ansatz, a widely used low-rank approximation of the wavefunction. Within the MPS ansatz, the wavefunction is rewritten as:

$$|\Psi\rangle = \sum_{n_1,\dots,n_L} A[1]^{n_1} A[2]^{n_2} \cdots A[L]^{n_L} |n_1,\dots,n_L\rangle.$$
 (4)

Each inner tensor A[i] (1 < i < L) is of order three, as illustrated in Fig. 1a. The superscript  $n_i$  denotes the physical index labeling the possible states at site i, and for each  $n_i$ , the component  $A[i]^{n_i}$  is a matrix of size  $\chi_i \times \chi_{i+1}$ . The parameter  $\chi_i$  represents the bond dimension between sites i-1 and i; in the following, we denote the maximum MPS bond dimension by M. The MPS representation offers a convenient ansatz for performing the low-rank approximation of the wavefunction. Controlled truncation of the MPS bonds via singular-value decomposition (SVD) can be applied directly to an existing MPS, a process justified by the Schmidt decomposition [21, 40], as depicted in Fig. 2. By employing such a truncation, the MPS ansatz can represent the quantum states more economically.

Alongside MPS, an analogous framework exists for operators: the matrix-product operator (MPO) formalism [21, 26, 27]:

$$\hat{O} = \sum_{m,n} W[1]^{m_1 n_1} W[2]^{m_2 n_2} \dots W[L]^{m_L n_L}$$

$$|m_1, \dots, m_L\rangle \langle n_1, \dots, n_L|.$$
(5)

For each site i, the local tensor  $W[i]^{m_i n_i}$  carries two physical indices  $(m_i, n_i)$  and can be viewed as a  $\beta_i \times \beta_{i+1}$ 

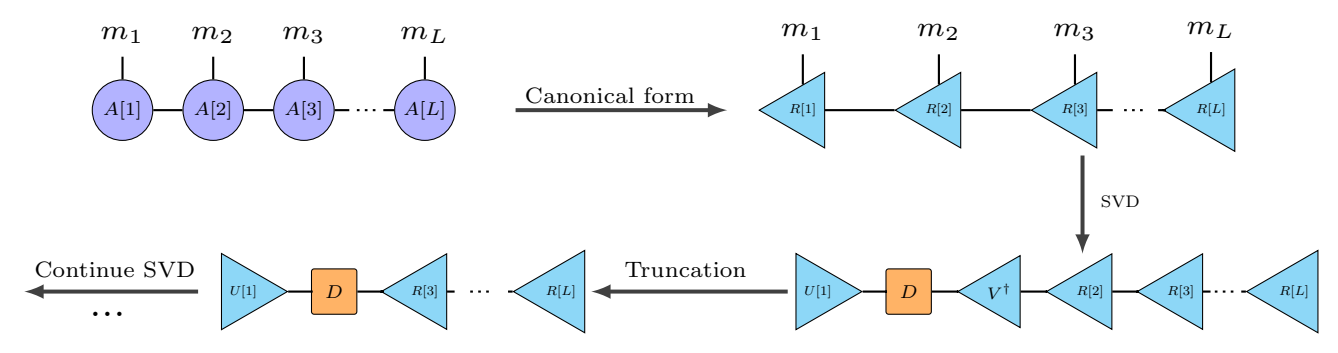


Figure 2: The classical SVD method to compress the MPS. First, the MPS is brought into right-canonical form via successive QR decompositions. Then, sweeping from left to right, we carry out SVDs at each site and truncate the smallest singular values. Finally, the S and  $V^{\dagger}$  matrices are merged into the next site.

matrix, where  $\beta_i$  is the MPO bond dimension between sites i-1 and i, as illustrated in Fig. 1b. We denote the largest of these bond dimensions by D. In Eq. (5), the operator  $\hat{O}$  is expressed as a summation of mappings from  $|n_1,\ldots,n_L\rangle$  to  $|m_1,\ldots,m_L\rangle$ , and the coefficients arise from contracting the chain of sequence of W matrices. The MPO representation can fully utilize the sparsity of the physical or chemical Hamiltonian by constructing it properly [26, 27, 41, 42]. For example, the Heisenberg XXZ model can be represented exactly as an MPO of small bond dimension D=5 [40], regardless of the system size.

As with a Hamiltonian operator acting on a state vector to produce another vector, applying an MPO to an MPS yields a new MPS by contracting the physical indices at each site [21]. Likewise, adding two MPS produces a new MPS; both operations lead to boosted bond dimensions. To keep subsequent calculations feasible and efficient, especially in iterative algorithms, it is crucial to compress the resulting MPS, as illustrated in Fig. 2. There are also alternative MPS compression methods, including the zip-up method [43], the density matrix method [44], and the variational method [21], each offering different trade-offs in accuracy, efficiency, and applicability. In this work, we employ the standard SVD method, which is the most controllable and accurate.

### C. The Lanczos algorithm with MPS

Since the Lanczos algorithm is inherently "matrix-free" and the MPS and MPO forms offer an economic way to represent Hamiltonians and states, it is reasonable to combine these tensor networks with the Lanczos algorithm [30].

As discussed before, the core step in the Lanczos algorithm is to compute new Krylov vectors via Eq. (1c). In the tensor network representation, the term  $H|v_i\rangle$  is realized by MPO-MPS multiplication, and the orthogonalization is implemented by MPS-MPS addition, leading to enlarged MPS bond dimension. As discussed, the MPS compression is needed to reduce the bond dimension back

to the capped one, introducing extra errors.

The first consequence of this MPS truncation error is the loss of orthogonality. Because Krylov vectors are computed iteratively from preceding vectors, round-off errors accumulate and break global orthogonality. Repeatedly applying the Gram-Schmidt procedure does not solve this issue, as new errors arise during the MPS-MPS addition and subsequent compression steps. Ultimately, this is addressed by the re-orthogonalization technique proposed in [30], which constructs a suitable linear combination of the current Krylov vectors so that the resulting vectors are well-orthogonalized:

$$|\psi_a\rangle = \sum_{i=0}^a C_{ai} |v_i\rangle \tag{6}$$

Note that we do not create new MPS for these orthogonal states  $\{|\psi_0\rangle, |\psi_1\rangle, |\psi_2\rangle, \dots\}$ ; instead, we leave the original MPS Krylov vectors  $\{|v_0\rangle, |v_1\rangle, |v_2\rangle, \dots\}$  unchanged, only solve the matrix C (by a Gram-Schmidt-like procedure) and utilize C in the following calculations. When calculating the effective Hamiltonian for the Lanczos algorithm, the matrix elements are calculated by:

$$\tilde{H}_{ab} = \langle \psi_a | H | \psi_b \rangle = \sum_{i=0}^{a} \sum_{j=0}^{b} C_{ai}^* C_{bj} \langle v_i | H | v_j \rangle.$$
 (7)

The Ritz pairs  $\{e_i, r_i\}$  are obtained by solving the effective Hamiltonian  $\tilde{H}$ , the actual Ritz vector is obtained by:

$$|R_i\rangle = \sum_{j=0}^{n-1} r_{ij} |\psi_j\rangle = \sum_{j=0}^{n-1} \sum_{k=0}^{j} r_{ij} C_{jk} |v_k\rangle,$$
 (8)

where n is the size of the current Krylov subspace. Any desired quantity, especially the expectation value  $\langle R_i | \hat{O} | R_i \rangle$  for an operator  $\hat{O}$ , can be computed from the summation of the terms  $\langle v_i | \hat{O} | v_j \rangle$ .

The second consequence of the MPS truncation error is the divergence from the desired Krylov space. Typically, only a small MPS bond dimension is needed to represent low-lying eigenstates, since the ground state obeys an area law for entanglement. However, a larger bond dimension is required to represent  $H | \psi \rangle$  if  $| \psi \rangle$  is an arbitrary state, even when  $| \psi \rangle$  itself can be approximated by an MPS with a small bond dimension [21, 35]. The reason is that the Hamiltonian H is typically a sum of operators, and applying it to  $| \psi \rangle$  can generate a more complex entanglement pattern, as each term introduces additional correlations that increase the overall entanglement in the resulting state.

Such an error prevents the Krylov vectors from "exploring" the Hilbert space correctly; the resulting Krylov space deviates further from the intended one, and newly generated Krylov vectors no longer provide additional independent information in subsequent iterations. Consequently, as displayed later in Sec. IV, the most significant result of this error is the severely broken convergence observed for most Hamiltonians.

In this work, we focus on strategies to mitigate the impact arising from the second consequence of MPS truncation errors, i.e., improving the convergence of the Lanczos algorithms.

# III. LANCZOS ALGORITHMS RESTARTED WITH MULTIPLE RITZ VECTORS

We first depict our primary improvement for the algorithm based on the above issues to enhance the convergence. The most straightforward way is to reduce the truncation error for the multiplication-compression  $H|\psi\rangle$ . Concretely, once convergence stalls, we restart the Lanczos procedure using the Ritz vector. After solving the effective Hamiltonian in Eq. (7) and obtaining a series of Ritz vectors via Eq. (8), we select the Ritz vector  $|R_0\rangle$  (when targeting the ground state) as the initial state to generate new Krylov vectors following Eq. (1) and re-run the standard Lanczos algorithm. The restart is repeated until the desired accuracy is obtained or the convergence can not be improved anymore. We will see in Sec. IV that this restart can significantly enhance the accuracy by several orders of magnitude. The essential intuition is that the Ritz vector  $|R_i\rangle$  is already close to an eigenstate. When generating the new Krylov vector, applying the Hamiltonian H to the approximate eigenstate  $|R_i\rangle$  leads to a resulting state that is still close to the eigenstate. According to the area law, a low-lying eigenstate is cheap to be represented by an MPS; therefore, only a small bond dimension is sufficient to represent  $H|R_i\rangle$ , which also indicates that the truncation will not cause a large error.

However, finding the ground state as an example, such a restart algorithm retains information only for the Ritz vector directly associated with the lowest Ritz value, which effectively limits the solution to the ground state. Therefore, the excited states must wait until the ground state is sufficiently converged, after which the first excited state can be computed by re-running the Lanczos algorithm from scratch, with all newly generated Krylov

states orthogonalized against the converged ground state. We recommend including the previous accurate states in the Krylov subspace (for computing the effective Hamiltonian) so that all the newly solved Ritz vectors are automatically orthogonalized to them. The total cost of the entire algorithm is, therefore, the sum of the individual costs required to compute each target state separately. Abandoning other Ritz vectors loses some advantages of the classical Lanczos procedure, where information from multiple Ritz vectors can collectively accelerate the convergence of other target states.

The next improvement we propose is to use the previously obtained information as much as possible. When targeting K eigenstates, we restart the Lanczos procedure with K Ritz vectors  $\mathcal{K}_0 = \{|R_0\rangle, |R_1\rangle, \ldots, |R_{K-1}\rangle\}$ , and therefore the Krylov subspace is spanned by  $\{\mathcal{K}_0, H\mathcal{K}_0, \ldots, H^{n-1}\mathcal{K}_0\}$ , where n determines the size of the subspace.

 ${\bf Algorithm~1~Lanczos~algorithms~restarted~with~multiple~Ritz~vectors}$ 

```
Input:
        Hamiltonian H as MPO, initial state \psi_0 as MPS
        K eigenpairs S = \{(\theta_i, |R_i\rangle)\}_{i=0}^{K-1} as MPS
 1: Initialize Q_0 = [\psi_0], \mathcal{S} = \emptyset, \mathcal{L} = \emptyset
 2: for i = 1, 2, \ldots, until convergence
 3:
          set Q = [Q_0]
 4:
          for j = 0, 1, \cdots until convergence
 5:
               Q_{i+1} = \text{Compressed } HQ_i
 6:
               Orthogonalize MPS in Q_{j+1}
 7:
               Append Q_{i+1} to Q
 8:
               Re-orthogonalize \mathcal{L} + \mathcal{Q}
               Solve Ritz values
 9:
10:
          end for
          Find K - |\mathcal{L}| Ritz pairs (\theta_k, R_k) of H in span(\mathcal{Q})
11:
          for k = 1, 2, ..., K - |\mathcal{L}|
12:
               if (\theta_i, R_i) \notin \mathcal{S} and ||(H - \theta_i I)R_i|| < \epsilon then
13:
                    set S = S \cup \{(\theta_i, \Psi_i)\}, \mathcal{L} = \mathcal{L} \cup \{R_i\}
14:
               end if
15:
16:
          end for
17:
          if |S| = K then
18:
               break
19:
          end if
          \mathbf{set}\ Q_0 = [R_{|\mathcal{L}|} \cdots R_{K-1}]
20:
21: end for
22: return S
```

As depicted in Alg. 1, after the first-stage Lanczos, we restart with the Ritz-vector set  $Q_0$ . Subsequent new Krylov vectors  $Q_1$  are generated by applying H on each Ritz vector, and orthogonalizing them against the two preceding Krylov vectors by the Gram-Schmidt process one by one. Repeating this process (applying H and orthogonalizing) iteratively builds the Krylov subspace. Both the orthogonalization by Eq. (1c) and the re-orthogonalization by Eq. (6) depend only on previous vectors. Hence, we can update the effective Hamiltonian by solely adding the new rows and columns corresponding to the latest Krylov vectors without disturbing

any existing Krylov vectors or matrix elements. It allows real-time monitoring of the convergence of the current Lanczos procedure. Once convergence stalls, we halt the current iteration and trigger the next restart.

Typically, the lowest-lying states (e.g., the ground state and first excited state) converge most rapidly, so it is unnecessary to include the collection  $\mathcal{L}$  of the "obtained" approximated eigenstates in the next restart. However, the truncation of the following calculations will introduce errors related to the ground state, so the orthogonalization against the obtained eigenstates can not be guaranteed. We can address this issue by always including these obtained vectors  $\mathcal{L}$  in the reorthogonalization process.

The idea is similar to the block Lanczos algorithm [15] in scientific computing to some extent, whose motivation is to improve the convergence for clustered eigenvalues and enrich the searching directions; therefore, our method also admits these advantages if we follow the block Lanczos algorithm strictly and initialize the algorithm with multiple initial states as well. In the textbook's standard methods, there are several popular restarted Lanczos algorithms, e.g., the explicitly restarted [45] and the implicitly restarted Lanczos algorithms [15, 20, 46]; but our practice indicates that neither helps improve accuracy.

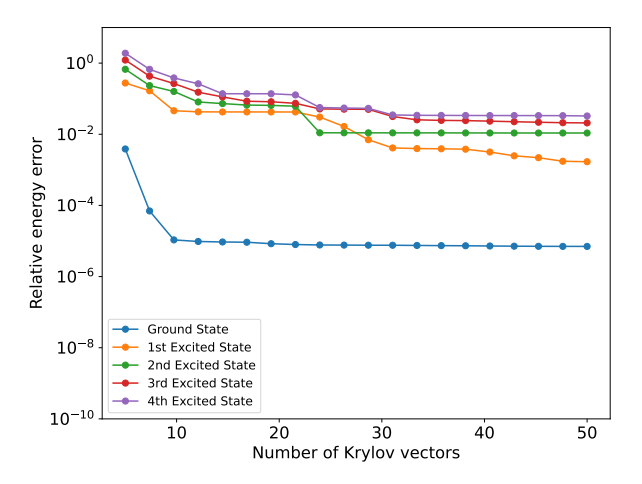


Figure 3: The convergence of the first five low-lying states for the Fermi-Hubbard model, when combining the MPS representation with the standard Lanczos algorithm. It performs mediocre except for the ground state, since the initial state is close to it.

### IV. BENCHMARK

To demonstrate the accuracy and efficiency of our method, we apply it to several Hamiltonians of broad interest in quantum many-body physics. We will also show that the numerical experiments are consistent with our physical intuition which drives our method's improvement. In the following, we denote the original Lanczos procedure employing MPS without any restarts

as the plain Lanczos method (PLM), the version that restarts with a single Ritz vector as the restarted Lanczos (RL), and our improved approach as the multistate restart Lanczos (MRL). The total computational cost scales with the number of Krylov vectors constructed, since both MPS multiplication—compression and effective-Hamiltonian evaluation depend directly on the count of these vectors. Henceforth, we shall interchange "number of steps," "number of iterations," and "Krylov vectors" to refer to this same quantity, which measures the computational cost.

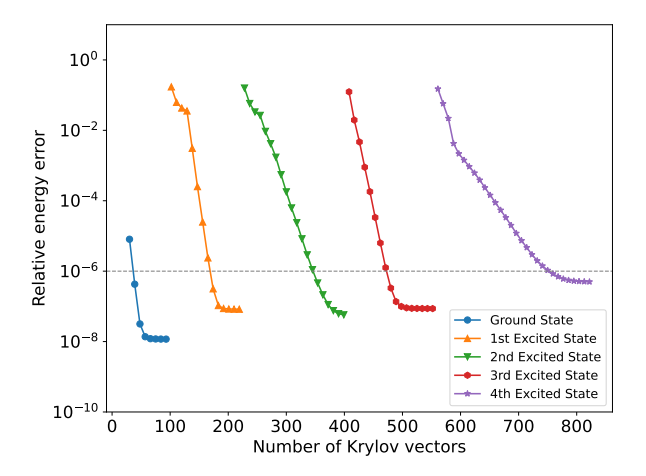


Figure 4: We can significantly improve the convergence by introducing a restart with a single Ritz vector. Since only one target state can be concentrated on at a time, we must wait until the previous eigenstate has been found before calculating the next one. Therefore, each target state is calculated independently, and the curves are separated. We restart the Lanczos procedure every ten steps. The x-axis denotes the cumulative number of Krylov vectors generated, reflecting the computational cost.

## A. The Fermi-Hubbard model

We first choose the Fermi-Hubbard model [47, 48], one of the most studied models in condensed matter physics. It describes the interaction of fermions on a lattice system, offering crucial insights into phenomena such as Mott insulating [49, 50] and high-temperature superconductivity [51–53]. The Fermi-Hubbard Hamiltonian is given by:

$$H_{\rm FH} = -t \sum_{\langle i,j \rangle,\sigma} (a_{i\sigma}^{\dagger} a_{j\sigma} + a_{j\sigma}^{\dagger} a_{i\sigma}) - \mu \sum_{i,\sigma} n_{i\sigma}$$
$$+ U \sum_{i} \left( n_{i\uparrow} - \frac{1}{2} \right) \left( n_{i\downarrow} - \frac{1}{2} \right),$$

where  $a_{i\sigma}^{\dagger}$  and  $a_{i\sigma}$  are fermionic creation and annihilation operators at site i with spin  $\sigma$ . We set the hopping amplitude to t = 1.0, the chemical potential to  $\mu = 0$  (half-filling), and the on-site interaction to U = 4.0. The number of lattice sites is L = 8, so it is convenient to

get the reference eigenpairs from exact diagonalization. We cap the Krylov vectors' bond dimension at 64, which means we always compress the MPS bond dimension to 64 after any operations (addition or multiplication). We initialize the calculation from the ground state of the non-interacting Fermi-Hubbard model (U=0), which is trivially inexpensive to obtain.

First, we present the energy errors for finding the first five low-lying eigenstates using the original plain Lanczos method (PLM). As illustrated in Fig. 3, the convergence stalls far from the reference values, in agreement with Sec. II C, where we interpreted that the original Lanczos algorithm fails to find the eigenstates accurately. The only exception is the ground state, which converges well since the initial state is very close to the ground state.

As a primary improvement discussed in Sec. II C, the Lanczos algorithm restarted (RL) with a single Ritz vector could improve the accuracy significantly by roughly three orders of magnitude, as shown in Fig. 4. However, even though such a simple restart scheme improves the accuracy dramatically, the convergence of the fourth excited state requires up to 250 iterations to reach its best accuracy, as shown in Fig. 4. That is because the gap between the fourth and the fifth excited state is much smaller than that of the previous eigenstates.

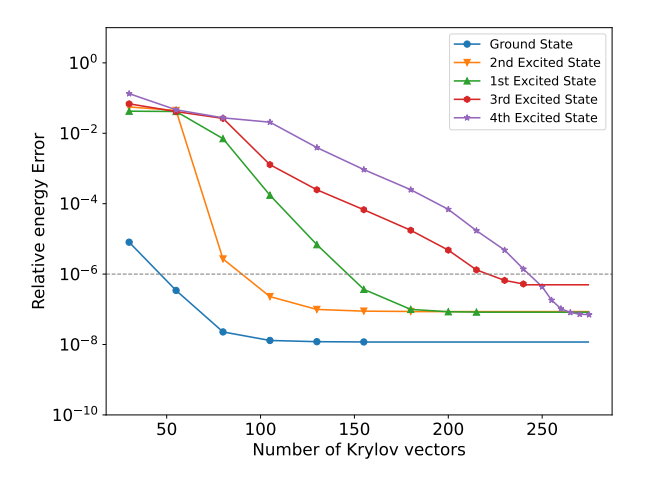


Figure 5: Finding low-lying states for the Fermi-Hubbard model when restarting with multiple Ritz vectors, which not only improves accuracy but also significantly reduces computational cost. We fix the size of the subspace as 35 for each restart, which means the Krylov subspace is spanned by  $\{\mathcal{K}_0, H\mathcal{K}_0, \dots, H^6\mathcal{K}_0\}$ , where  $\mathcal{K}_0$  is the Ritz vector collection from the last restart.

In effect, such a simple restart can be viewed as a special case of the explicitly restarted Lanczos algorithm, where we set the weight for all other Ritz vectors to zero. Since the limited bond dimension can only carry limited information, only such an extremely biased weight setting could keep meaningful. Consequently, such a simple restart can only keep the information from one Ritz vector, and thus incurs a very high computational cost since all other useful information stored in other Ritz vectors

is abandoned.

By incorporating multiple Ritz vectors in the procedure, the multi-state restart Lanczos (MRL) cuts the computational cost by two-thirds. As shown in Fig. 5, although the convergence of any single state may appear slower, all target states converge in parallel. Thanks to cross–state assistance, all five Ritz states reach relative energy error on the order of  $10^{-6}$  (or better) within only 250 iterations, whereas RL requires 250 Krylov vectors merely to converge the fourth eigenstate.

## B. The spin-1/2 Heisenberg XXZ model in a longitudinal magnetic field

The second model we chose is the one-dimensional spin-1/2 Heisenberg XXZ model [54–58] in a uniform longitudinal magnetic field [59]:

$$H_{XXZ} = J \sum_{\langle i,j \rangle} \frac{1}{2} (S_i^+ S_j^- + S_i^- S_j^+) + \Delta \sum_{\langle i,j \rangle} S_i^z S_j^z - h \sum_i S_i^z$$
(9)

to benchmark our algorithm. We denote  $S_j^\pm = S_j^x \pm i\,S_j^y$  operators as raising/lowering operators, and  $S_i^\alpha = \frac{1}{2}\,\sigma_i^\alpha$  is the local spin- $\alpha$  operator at site i, where  $\sigma_i^\alpha$  is the Pauli  $\alpha$  matrix. We set the nearest-neighbor exchange coupling strength to J=0.8, the anisotropy parameter to  $\Delta=0.9$ , and the uniform magnetic field strength to h=0.1. The number of lattice sites is L=16; we cap the Krylov vectors' bond dimension at 32. The zero total spin is broken due to the positive magnetic field; therefore, we target the low-lying eigenstates for total spin  $S_z=1$ , and the initial state is set as a random state satisfying this total spin.

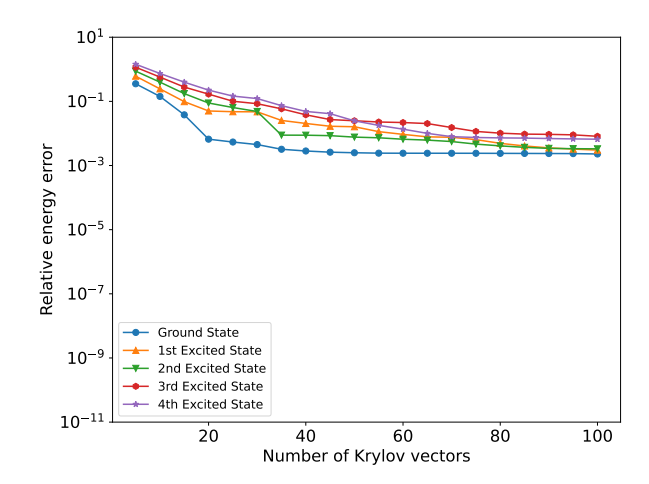


Figure 6: When using the PLM to simulate the Heisenberg model, the convergence stalls far away from the reference eigenvalues.

As in the previous example, the PLM fails to find the eigenstates, as shown in Fig. 6. Although the restart

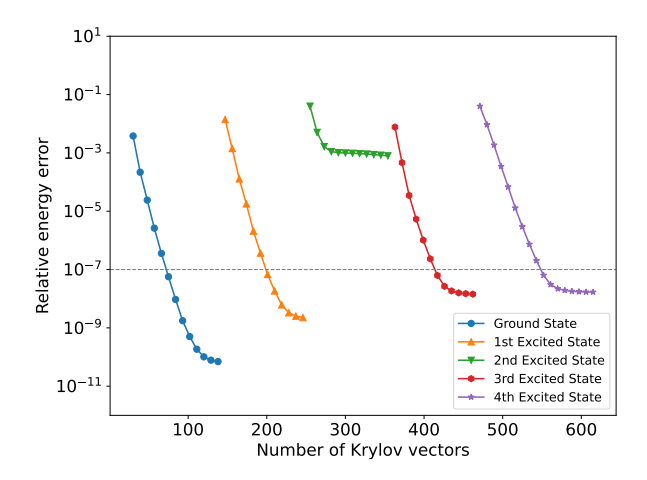


Figure 7: For each restart step, the subspace size is set to 10. Even though the accuracy is improved by RL, the second excited state still can not be computed accurately.

Lanczos (RL) boosts accuracy by roughly seven orders of magnitude for most of the target states, its convergence for the second excited state remains unsatisfactory, as illustrated in Fig. 7. In contrast, our multi-state restart Lanczos (MRL) recovers all five eigenstates in fewer than 300 iterations, i.e., under 300 Krylov vectors need to be generated (Fig. 8). Moreover, the second excited state can be found accurately using the same initial state as RL. That is because the information from other Ritz vectors enhances the convenience for each other. This indicates that by introducing more Ritz vectors in the iteration, MRL accelerates convergence and improves accuracy beyond what RL achieves with a single Ritz vector.

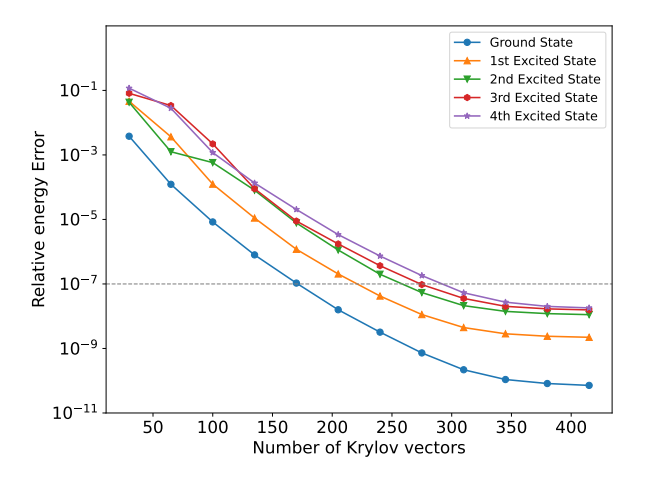


Figure 8: MRL succeeds where RL falters, accurately finding the eigenstates that RL cannot. The second excited state of the Heisenberg Hamiltonian in an external field is accurately found, and all target states achieve relative errors below  $10^{-7}$  within 300 iterations.

In computational physics and numerical linear algebra, the accuracy of approximate eigenstates can be assessed by evaluating the energy variance [1, 36, 60, 61],

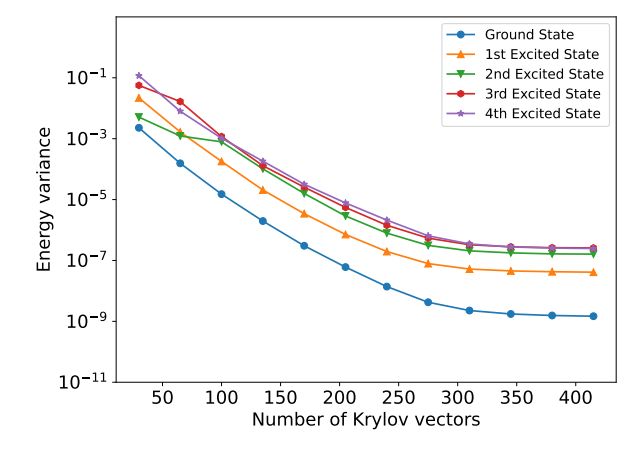


Figure 9: The energy variance can also faithfully describe how close the approximate eigenstates are to the exact eigenstates.

also known as the residual variance. The energy variance of an approximate eigenpair  $(\theta_i, |R_i\rangle)$  with respect to a Hamiltonian H is given by:

$$\sigma^2 = \langle R_i | (H - \theta_i I)^2 | R_i \rangle, \qquad (10)$$

which measures how closely the approximate eigenvalue  $\lambda$ and eigenstate  $|\psi\rangle$  approximate an exact eigenpair. Minimizing this variance is essential in iterative eigenvalue algorithms such as Lanczos and Davidson methods to achieve reliable convergence [60]. Here, we also examine the consistency of the relative energy error and energy variance. To lower the computational cost of Eq. (10), we avoid explicitly forming  $(H - \theta_i I)^2 |R_i\rangle$ . Instead, we evaluate the energy variance directly via tensor-network contractions, analogous to that employed in the DMRG algorithm [21, 26]. As presented in Fig. 9, the curve and the magnitude order of energy variance correspond well to those of the relative energy error. Using energy variance as an error metric has the advantage of requiring no reference values, allowing us to measure errors when calculating large systems whose exact eigenvalues are difficult to obtain. In the following part of this work, we will use the energy variance as the metric of errors.

To examine the scalability of our method, we increase the system size to L=30 while capping the bond dimension of Krylov vectors at 128. As presented in Fig. 10, all five target states converge to energy variance below  $10^{-5}$  before 350 iterations, which corresponds to a relative energy error of approximately  $10^{-7}$ , as inferred from the comparison between Fig. 8 and Fig. 9. This indicates that our MRL is a scalable and reliable method for finding low-lying states.

### V. CONCLUSION AND DISCUSSION

In this work, we dramatically improve the convergence of the Lanczos algorithm when paired with MPS representations by introducing targeted modifications that

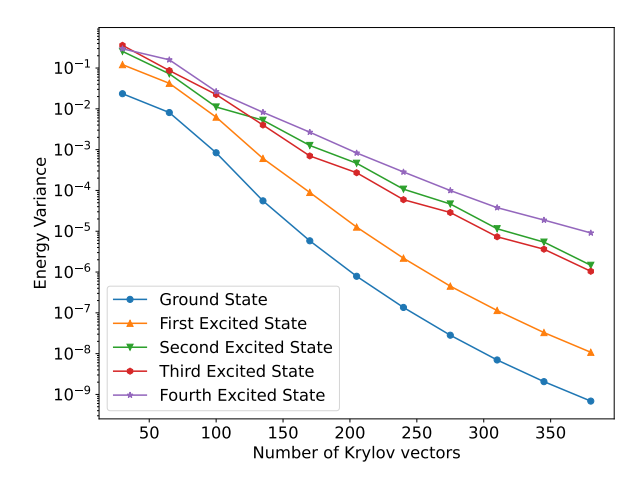


Figure 10: Convergence of MRL for finding the low-lying states of the Heisenberg XXZ model.

aim at reducing truncation errors, which are the principal source of inaccuracy in the MPS-based Lanczos method. Inspired by the area law, we leverage the insight that applying the Hamiltonian to approximate eigenstates (Ritz vectors) can be faithfully captured with relatively small MPS bond dimensions. Embedding this insight into the Lanczos restart procedure dramatically reduces truncation errors, thereby boosting accuracy and convergence. We demonstrated the efficiency of our method by benchmarking on the Fermi-Hubbard model and the Heisenberg model in a longitudinal field, and demonstrated its scalability on a larger system. We expect our improved Lanczos algorithm to serve as a valuable complement or alternative to the DMRG algorithm, especially for finding low-lying excited states. Because the method relies only on standard MPO-MPS multiplication, MPS addition, and compression, it can be integrated into any modern tensor-network library without additional heavy infrastructure. Moreover, it is not confined to the MPS/MPO framework; any ansatz supporting these operations (e.g., projected entangled pair states (PEPS) [62], tree tensor network states (TTNS) [63], isometric tensor-network states (isoTNS) [64], and so on) can be incorporated into our MRL.

- [1] C. Lanczos, An iteration method for the solution of the eigenvalue problem of linear differential and integral operators, J. Res. Nat. Bur. Stand. 45, 255 (1950).
- [2] S. R. White, Density matrix formulation for quantum renormalization groups, Phys. Rev. Lett. **69**, 2863 (1992).
- [3] P. Prelovšek and J. Bonča, Strongly Correlated Systems: Numerical Methods (Springer, Berlin, 2013).
- [4] A. W. Sandvik, Finite-size scaling of the ground-state parameters of the two-dimensional heisenberg model, Phys. Rev. B 56, 11678 (1997).
- [5] J. Haegeman, S. Arunachalam, T. J. Osborne, et al., Tensor network algorithms: A route map, Annu. Rev. Condens. Matter Phys. 13, 73 (2022).
- [6] J. Jaklič and P. Prelovšek, Lanczos method for the calculation of finite-temperature quantities in correlated systems, Phys. Rev. B 49, 5065 (1994).
- [7] S. Sugiura and A. Shimizu, Canonical thermal pure quantum state, Phys. Rev. Lett. 111, 010401 (2013).
- [8] J. Jaklič and P. Prelovšek, Finite-temperature properties of doped antiferromagnets, Adv. Phys. **49**, 1 (2000).
- [9] V. Laguta, Y. O. Zagorodniy, R. Kuzian, I. Kondakova, V. Chlan, R. Řezníček, H. Štěpánková, D. Bohdanov, J. Hlinka, and R. Ramesh, Low-temperature ground state structure of pbti o 3, Phys. Rev. B 107, 104107 (2023).
- [10] E. R. Gagliano and C. A. Balseiro, Dynamical properties of quantum many-body systems at zero temperature, Phys. Rev. Lett. 59, 2999 (1987).
- [11] P. Pavlov, A. Smith, L. Z. Tan, et al., Unravelling quantum dynamics using flow equations, Nat. Phys. 10.1038/s41567-024-02549-2 (2024).
- [12] S. Sun, M. Motta, R. N. Tazhigulov, A. T. K. Tan, G. K. Chan, and A. J. Minnich, Quantum computation of finite-temperature static and dynamical properties of spin systems using quantum imaginary time evolution, PRX Quantum 2, 010317 (2021).

- [13] C. C. Paige, Computational variants of the lanczos method for the eigenproblem, J. Inst. Math. Appl. 10, 373 (1972).
- [14] J. K. Cullum and R. A. Willoughby, Lanczos algorithms for large symmetric eigenvalue computations: Volume I: Theory, Progress in Scientific Computing, Vol. 3 (Birkhäuser Boston, Boston, MA, 1985).
- [15] Z. Bai, J. Demmel, J. Dongarra, A. Ruhe, and H. van der Vorst, Templates for the solution of algebraic eigenvalue problems: a practical guide (SIAM, 2000).
- [16] A. Bhattacharya, P. Nandy, P. P. Nath, and H. Sahu, On krylov complexity in open systems: an approach via bi-lanczos algorithm, J. High Energy Phys. 2023 (12), 066.
- [17] P. Weinberg and M. Bukov, Quspin: a python package for dynamics and exact diagonalisation of quantum many body systems. part ii: bosons, fermions and higher spins, SciPost Phys. 7, 020 (2019).
- [18] A. M. Läuchli, J. Sudan, and R. Moessner, The s=1/2 kagome heisenberg antiferromagnet revisited, Phys. Rev. B **100**, 155142 (2019).
- [19] S. Iskakov and M. Danilov, Exact diagonalization library for quantum electron models, Comput. Phys. Commun. 225, 128 (2018).
- [20] R. B. Lehoucq, D. C. Sorensen, and C. Yang, ARPACK Users' Guide: Solution of Large-Scale Eigenvalue Problems with Implicitly Restarted Arnoldi Methods, Software, Environments & Tools, Vol. 6 (Society for Industrial and Applied Mathematics, 1998).
- [21] U. Schollwöck, The density-matrix renormalization group in the age of matrix product states, Annals of Physics **326**, 96 (2011).
- [22] J. C. Bridgeman and C. T. Chubb, Hand-waving and interpretive dance: An introductory course on tensor networks, J. Phys. A: Math. Theor. 50, 223001 (2017).

- [23] S. Östlund and S. Rommer, Thermodynamic limit of density matrix renormalization, Phys. Rev. Lett. 75, 3537 (1995).
- [24] S. Rommer and S. Ostlund, Class of ansatz wave functions for one-dimensional spin systems and their relation to the density matrix renormalization group, Phys. Rev. B 55, 2164 (1997).
- [25] H. Ma, U. Schollwöck, and Z. Shuai, Density Matrix Renormalization Group (DMRG)-Based Approaches in Computational Chemistry (Elsevier, 2022).
- [26] G. K. Chan, A. Keselman, N. Nakatani, Z. Li, and S. R. White, Matrix product operators, matrix product states, and ab initio density matrix renormalization group algorithms, J. Chem. Phys. 145 (2016).
- [27] S. Keller, M. Dolfi, M. Troyer, and M. Reiher, An efficient matrix product operator representation of the quantum chemical Hamiltonian, J. Chem. Phys. 143, 244118 (2015).
- [28] S. R. White, Density matrix renormalization group algorithms with a single center site, Phys. Rev. B 72, 180403 (2005).
- [29] R. N. Pfeifer, Symmetry-protected local minima in infinite DMRG, Phys. Rev. B 92, 205127 (2015).
- [30] P. E. Dargel, A. Woellert, A. Honecker, I. McCulloch, U. Schollwöck, and T. Pruschke, Lanczos algorithm with matrix product states for dynamical correlation functions, Phys. Rev. B 85, 205119 (2012).
- [31] A. Dektor, P. DelMastro, E. Ye, R. Van Beeumen, and C. Yang, Inexact subspace projection methods for low-rank tensor eigenvalue problems, arXiv preprint arXiv:2502.19578 10.48550/arXiv.2502.19578 (2025).
- [32] R. Haydock, The recursive solution of the Schrödinger equation, Solid State Phys. 35, 215 (1980).
- [33] J. Laflamme Janssen, B. Rousseau, and M. Côté, Efficient dielectric matrix calculations using the lanczos algorithm for fast many-body  $g_0w_0$  implementations, Phys. Rev. B **91**, 125120 (2015).
- [34] H.-G. Weikert, H.-D. Meyer, L. Cederbaum, and F. Tarantelli, Block lanczos and many-body theory: Application to the one-particle green's function, J. Chem. Phys. 104, 7122 (1996).
- [35] S. Paeckel, T. Köhler, A. Swoboda, S. R. Manmana, U. Schollwöck, and C. Hubig, Time-evolution methods for matrix-product states, Annals of Physics 411, 167998 (2019).
- [36] G. H. Golub and C. F. Van Loan, *Matrix Computations* (Johns Hopkins University Press, 2013).
- [37] E. Dagotto, Correlated electrons in high-temperature superconductors, Rev. Mod. Phys. 66, 763 (1994).
- [38] S. Östlund and S. Rommer, Thermodynamic limit of density matrix renormalization, Phys. Rev. Lett. 75, 3537 (1995).
- [39] S. Rommer and S. Östlund, Class of ansatz wave functions for one-dimensional spin systems and their relation to the density matrix renormalization group, Phys. Rev. B 55, 2164 (1997).
- [40] J. Hauschild and F. Pollmann, Efficient numerical simulations with tensor networks: Tensor Network Python (TeNPy), SciPost Phys. Lect. Notes , 5 (2018).
- [41] J. Ren, W. Li, T. Jiang, and Z. Shuai, A general automatic method for optimal construction of matrix product operators using bipartite graph theory, J. Chem. Phys. 153 (2020).

- [42] H. Çakır, R. M. Milbradt, and C. B. Mendl, Optimal symbolic construction of matrix product operators and tree tensor network operators, arXiv preprint arXiv:2502.18630 10.48550/arXiv.2502.18630 (2025).
- [43] E. M. Stoudenmire and S. R. White, Minimally entangled typical thermal state algorithms, New J. Phys. 12, 055026 (2010).
- [44] L. Ma, M. Fishman, E. M. Stoudenmire, and E. Solomonik, Approximate Contraction of Arbitrary Tensor Networks with a Flexible and Efficient Density Matrix Algorithm, Quantum 8, 1580 (2024).
- [45] M. Szularz, J. Weston, M. Clint, and K. Murphy, A highly parallel explicitly restarted lanczos algorithm, in Applied Parallel Computing. Industrial Computation and Optimization, Lecture Notes in Computer Science, Vol. 1184 (Springer, Berlin, Heidelberg, 1996) pp. 651–660.
- [46] D. Calvetti, L. Reichel, and D. C. Sorensen, An implicitly restarted lanczos method for large symmetric eigenvalue problems, Electronic Transactions on Numerical Analysis 2, 1 (1994).
- [47] J. Hubbard, Electron correlations in narrow energy bands, Proc. R. Soc. Lond. A 276, 238 (1963).
- [48] A. Georges, G. Kotliar, W. Krauth, and M. J. Rozenberg, Dynamical mean-field theory of strongly correlated fermion systems and the limit of infinite dimensions, Rev. Mod. Phys. 68, 13 (1996).
- [49] R. Jördens, N. Strohmaier, K. Günter, H. Moritz, and T. Esslinger, A mott insulator of fermionic atoms in an optical lattice, Nature 455, 204 (2008).
- [50] C. Hofrichter, L. Riegger, F. Scazza, M. Höfer, D. Rio Fernandes, I. Bloch, and S. Fölling, Direct probing of the mott crossover in the su(n) fermi-hubbard model, Phys. Rev. X 6, 021030 (2016).
- [51] P. W. Anderson, The resonating valence bond state in La<sub>2</sub>CuO<sub>4</sub> and superconductivity, Science 235, 1196 (1987).
- [52] D. J. Scalapino, J. Loh, E., and J. E. Hirsch, d-wave pairing near a spin-density-wave instability, Phys. Rev. B 34, 8190 (1986).
- [53] E. Dagotto, Correlated electrons in high-temperature superconductors, Rev. Mod. Phys. 66, 763 (1994).
- [54] W. Heisenberg, Zur theorie des ferromagnetismus, Zeitschrift für Physik 49, 619 (1928).
- [55] C. N. Yang and C. P. Yang, One-dimensional chain of anisotropic spin-spin interactions. i. proof of bethe's hypothesis for the ground state in a finite system, Phys. Rev. 150, 321 (1966).
- [56] C. N. Yang and C. P. Yang, One-dimensional chain of anisotropic spin-spin interactions. ii. properties of the ground-state energy per lattice site for an infinite system, Phys. Rev. 150, 327 (1966).
- [57] F. C. Alcaraz, M. N. Barber, M. T. Batchelor, R. J. Baxter, and G. R. W. Quispel, Surface exponents of the quantum xxz, ashkin–teller and potts models, J. Phys. A: Math. Gen. 20, 6397 (1987).
- [58] B. Bertini, M. Collura, J. De Nardis, and M. Fagotti, Transport in out-of-equilibrium xxz chains: Exact profiles of charges and currents, Phys. Rev. Lett. 117, 207201 (2016).
- [59] M. V. Rakov and M. Weyrauch, Spin-1/2 xxz heisenberg chain in a longitudinal magnetic field, Phys. Rev. B 100, 134434 (2019).
- [60] J. K. Cullum and R. A. Willoughby, *Lanczos Algorithms* for Large Symmetric Eigenvalue Computations (SIAM,

- 2002).
- [61] R. M. Martin, *Electronic Structure: Basic Theory and Practical Methods* (Cambridge University Press, 2004).
- [62] F. Verstraete, M. M. Wolf, D. Pérez-García, and J. I. Cirac, Criticality, the area law, and the computational power of projected entangled pair states, Phys. Rev. Lett.
- **96**, 220601 (2006).
- [63] Y.-Y. Shi, L.-M. Duan, and G. Vidal, Classical simulation of quantum many-body systems with a tree tensor network, Phys. Rev. A 74, 022320 (2006).
- [64] M. P. Zaletel and F. Pollmann, Isometric tensor network states in two dimensions, Phys. Rev. Lett. 124, 037201 (2020).